https://doi.org/10.52131/jee.2022.0302.0027

*i*RASD Journal of Energy & Environment

Volume 3, Number 2, 2022, Pages 72 - 89

Journal Homepage:
https://journals.internationalrasd.org/index.php/jee

Microbial Growth Rate Kinetics in Biogas Production by Anaerobic Digestion of Chicken Manure

Abdulhalim Musa Abubakar[1], Kiman Silas[2], Mohammed Modu Aji[3], Usman H. Taura[4], Jerome Undiandeye[5]

[1] Department of Chemical Engineering, Faculty of Engineering, Modibbo Adama University (MAU), Yola, Nigeria. Email: abdulhalim@mau.edu.ng
[2] Department of Chemical Engineering, Faculty of Engineering, University of Maiduguri (UNIMAID), Borno State, Nigeria. Email: silaskiman@unimaid.edu.ng
[3] Department of Chemical Engineering, Faculty of Engineering, University of Maiduguri (UNIMAID), Borno State, Nigeria. Email: ajimohammed@ymail.com
[4] Department of Chemical Engineering, Faculty of Engineering, University of Maiduguri (UNIMAID), Borno State, Nigeria. Email: usmantaura@gmail.com
[5] Department of Chemical Engineering, Faculty of Engineering, University of Port Harcourt (UNIPORT), Rivers State, Nigeria. Email: jerome.undiandeye@uniport.edu.ng

ARTICLE INFO

Article History:
Received: October 08, 2022
Revised: December 10, 2022
Accepted: December 13, 2022
Available Online: December 15, 2022

Keywords:
Kinetic parameter
Chicken manure
Biogas
Anaerobic digestion
Growth kinetics
Bioenergy
Substrate concentration

JEL Classification Codes:
Q42, L95

Funding:
This research received no specific grant from any funding agency in the public, commercial, or not-for-profit sectors.

ABSTRACT

Kinetic study of microorganism's growth in chicken manure (CM) when producing biogas is often studied for scale-up purposes. CM are considered as waste, and can cause serious environmental consequences when not properly disposed. The objective of the study is to know the characteristics of the bioreactor condition or environment responsible for CM degradation and biogas production. Methods involves serial dilution, pour plating, cell count and the determination of Monod parameters. POLYMATH regression results shows that CM of particle density 0.0163 g/cm3 gives a maximum specific growth rate, μ_max of 0.007316 hr^(-1) and half saturation constant, K_s of 3.8× 〖10〗 ^8mg/l which points to substrate sufficiency for the survival of microorganisms and biogas production.

Corresponding Author's Email: silaskiman@unimaid.edu.ng
Citation: Abubakar, A. M., Silas, K., Aji, M. M., Taura, U. H., & Undiandeye, J. (2022). Microbial Growth Rate Kinetics in Biogas Production by Anaerobic Digestion of Chicken Manure. *IRASD Journal of Energy & Environment*, *3*(2), 72–89. https://doi.org/10.52131/jee.2022.0302.0027

1. Introduction

In CM, there are different types of micro-organisms, namely, *Salmonella spp.*, *Escherichia coli* (*E. coli*), and *Cryptosporidium*, to mention a few (Nauanova et al., 2020; Sule et al., 2019; Tian et al., 2023). During anaerobic batch fermentation of CM, these microorganisms grow under a variety of physical, chemical, and nutritional conditions. They do so by extracting nutrients from the medium (CM slurry) and converting them into biological compounds. According to UlukardeŞler & Atalay (2018), the kinetics of the growth of microorganisms can be investigated in two ways. One, is to measure the substrate concentrations during an experiment, a procedure that is tiring and consumes a lot of time. The second way is however, easier and faster. It entails measuring the gas production rates

in the course of the synthesis. Clearly, microbial growth and substrate consumption rates are two parameters that kinetic models on anaerobic digestion (AD) focuses on (Tena et al., 2021).

For bioreactors operating in batch mode, the kinetics of biogas production is proportional to specific growth rate of methanogenic bacteria inside the digester (Noori & Ismail, 2019; Venkateshkumar et al., 2020). Two types of bacterial growth models can be distinguished (González-figueredo et al., 2018): Structured Kinetic Models (SKMs) describing changes in cell population and classified into chemically structured models, morphologically structured models and, genetically structured models and, Unstructured Kinetic Models (UKMs) representing the metabolic behaviour of the biomass cell production. The significance of these growth models are to estimate the growth of microorganisms under environmental conditions (Hawkins et al., 2019), predict the behaviour of biochemical reactions (González-figueredo et al., 2018), assist engineers to design and control biological processes (Muloiwa et al., 2020) and, to determine the performance parameters influencing the product yield (Gallipoli et al., 2020).

Agarry et al. (2010) used Moser, Eckenfelder, Monod and the Adapted Miura models to determine the parameters K_s and μ_{max} using synthetic phenol in water as limiting substrate from different initial substrate concentration, S_o and carrying out model fitting, where results show that the Adapted Miura model gave the best fit. The Monod parameters estimated in the same author's work for an $S_o = 100$mg/l was K_s =23.8mg/l and μ_{max} =0.145 mg/mg/h and for an increase to $S_o = 200$mg/l shows an increase in K_s to 79.8mg/l and a decrease in μ_{max} to 0.120 mg/mg/h. The use of Monod kinetic models to study microbial behavior in CM is hardly researched; but Jaman et al. (2022) and Seekao et al. (2021) were able to study the kinetics of co-digested feedstock with CM. Because in some occasions, co-digestion is carried out to improve digestate quality for agricultural application (Johari et al., 2023). For instance, anaerobic co-digestion of pig fat/piggery waste and CM contributed to obtainable energy rise and enhanced biogas production with increasing organic loading rate (Buivydas et al., 2022; Olukanni & Ojukwu, 2021). Previous findings shows that additives such as magnetide, granular activated carbon and biochar had also proven to be an effective enhancers that are suitable for maintaining a desired environment for CM undergoing decay, even though co-feedstock of a primary substrate selected for digestion is often seen as an additive too (Alskory et al., 2021; Cahyono et al., 2023; Ziganshina & Ziganshin, 2022). Typically, addition of solid residue (hydrochar) to anaerobic reactors digesting CM improves methane yield by 14.1%, as obtained in Hurst et al. (2022). Objectives of this study therefore, are to determine the cell population in form of colonies inside a CM sample undergoing anaerobic fermentation using pour plate method, use kinetics to describe the behavior of substrate and microorganisms involved in the process, and to justify this behavior using the generic Monod equation after estimating their kinetic parameters.

2. Methodology

2.1 Feedstock Characterization

CM was obtained from the poultry farm of the University of Maiduguri was collected. Traditional hand-picking method was employed to remove other impurities from the CM, apart from other existing treatment strategies like pyrolysis, gasification, composting, torrefaction and hydrothermal liquification described in Manogaran et al. (2022). In this work, moisture content (MC) was calculated according to equation given by Matheri et al. (2017) while total solids (TS)/organic matter (OM) content, carbon-to-nitrogen (C/N) ratio and ash content (AC) on wet basis were according to Najafi et al. (2019) and the American Society for Testing and Materials (ASTM) standard test method for ash content respectively. OM content and particle density (PD) were based on Ksheem (2015) and volatile solid (VS) content was determined based on the American Public Health Association (APHA) standard method.

2.2 Digester

2.2.1 Digester Start-Up

Using a digital weighing balance, 7.2 kg of dried CM was measured and mixed thoroughly with 7.05 kg of water (H_2O) to keep the substrate-to-H_2O ratio at 1:1.05; approximately equal to 1:1 (according to literature study). Substrate concentration, S, is the amount of substrate present that can be converted to product. With known mass of CM and known volume of H_2O (i.e., 0.00756m^3 taking 1000 kg/m^3 as density of H_2O), the initial substrate concentration, S_o, was calculated based on Equation 1:

$$\mathrm{S_o} = \frac{\text{amount of sample}}{\text{amount of } \mathrm{H_2O}} \quad (1)$$

S_o was used to estimate the biomass-to-substrate yield, $\mathrm{Y_{X/S}}$, of the digestion process as it is an important constant parameter. The initial pH and temperature of the mixture were measured using a 2601 pH/temperature meter before injecting into the batch digester (see Figure 1) via the top inlet using a funnel and closed tightly. The bottom outlet of the digester was kept closed and the gas pipe and gas holder were connected to hold the generated gas. A clamp was put mid-way close to the top of the narrow gas outlet pipe to prevent the generated biogas from entering the gas holder. The biodigester was then kept at the surrounding temperature. This digester technology is simple and peculiar to other technologies listed by Buivydas et al. (2022), for constructing anaerobic digesters for either CM or majority of other feedstock. A new technology coupling leach bed reactors and continuous stirred tank reactor (LBR-CSTR) is economically feasible for the digestion of CM coming with several important benefits (Kalogiannis et al., 2022).

2.3 Microbial Count

2.3.1 Determination of Microbial Concentration

To determine the initial cell or biomass concentration, X_o, 5ml of mixed sample was collected and charged into a small bottle and closed tightly. X_o was used together with S_o when computing $\mathrm{Y_{X/S}}$ and procedures taken to obtain X_o at t = 0 is based on the serial dilution prior to the pour plate method of cell concentration (X) measurement, according to Equation 2 (Okpokwasili & Nweke, 2005; Shariful Islam et al., 2021).

$$\mathrm{Y_{X/S}} = \frac{\text{g cell mass produced}}{\text{g substrate consumed}} = -\frac{\Delta \mathrm{X}}{\Delta \mathrm{S}} = \frac{\mathrm{X}-\mathrm{X_o}}{\mathrm{S}-\mathrm{S_o}} \quad (2)$$

The bacterial concentration was observed to decrease with respect to time and subsequent values were determined repeating the same step. It has also been reported by Haleem et al. (2013) that a number of microbes are present in poultry meats and procedures followed to determine these microbial contents was similar to the one explained here.

2.3.2 Serial Dilution

For accuracy, triplicates of experiment were carried out using the serial dilution procedure for the 5ml of sample taken. This was carried out using 9 test tubes lined in a rack for a single run of serial dilution experiment (SDE). The test tubes were washed and allowed to dry. The run serial dilutions were labelled 1, 2 and 3, each consisting of 9 test tubes filled with 9ml each of H_2O using a syringe. Three syringes were taken and labelled according to the run of serial dilutions (i.e. syringe 1 for run 1, 2 for 2 and syringe 3 for 3). Syringe 1, 2 and 3 was used to transfer CM slurry, drawing 1 ml each from the bottle containing 5ml of sample to the first test tube in the respective run of experiment. Contamination of bacteria between the runs is eminent if a single syringe is used and may affect data precision. In Run 1 (or SDE1), holding the first tube at an angle, it was shaked thoroughly by flicking vigorously with the index finger. This is referred to as the first dilution and was calculated using Equation 3 according to Reynolds (2016).

$$\text{Dilution Factor(DF)} = \frac{\text{Final volume } (V_f)}{\text{Initial volume } (V_i)} = \frac{(\text{Amount transfered}) + (\text{Diluent volume})}{\text{Amount transfered}} \quad (3)$$

DF for the first dilution is therefore called the 10^1 dilution, and is same for other tubes in SDE2 and SDE3. Using syringe 1 for SDE1, 1ml was transferred from the first test tube to the next test tube. This is called the 10^2 dilution; as total dilution is equal to current dilution multiplied by the previous dilution. The transfer was done up to the last (or 9th tube) in SDE1, summing up DF to 10^9 Total Dilutions Factor (TDF). For the other two SDEs, their respective syringe (2 and 3) was used to repeat the process, making sure each tube was shaked well before every transfer. Method used in this work doesn't take the average number of colonies from the last three tubes as reported by Reynolds (2016) but is assumed to be much similar given that the target is also the average number of colonies.

2.3.3 Preparation of Culture Media

Based on the Swe Biotech Nutrient Agar (NA) manual, 500 ml of distilled H_2O was poured to a graduated cylinder. Measurement of 15.7g of powdered NA to a 500 ml transparent bottle was carried out. From the graduated cylinder, 500 ml of distilled H_2O was added to the NA bottle after which the formation of visible clumps was observed. The solution was stirred by raising the bottle with both hands, swirling to break down all visible clumps before covering it tight. In order to ensure proper dissolution of agar in H_2O and also sterilize the media, it had to be autoclaved. Thus, sterile H_2O was first poured in an autoclave to the level of the indicator line and the NA bottle was placed inside and lid covered tightly. The autoclave was set to temperature of 121℃ and heated until the pressure gauge reads a 0 psi after which the bottle was removed. The melted agar was allowed to cool to about 45℃ in a water bath. Normally, if the liquid agar is too hot, certain bacteria are killed automatically, and if very cold, it will solidify in the bottle or as it is poured into petri dishes or plates. Hence, serial dilution was carried out prior to media preparation so that the agar is used immediately it cools to 45℃.

2.3.4 Pour Plate Technique

After the dilutions, 1 ml of inoculum was transferred to the empty sterile dishes from the ninth tube of each run using a labelled syringe. The pour plate method using serial dilution is normally a method used for quantifying bacteria in a given sample. The method was carried out by pouring the prepared media into the 3 plates by first flaming the mouth of the vessel, making sure it covers the entire bottom surface of the plate and lastly covering the plates. The poured plates were gently swirled for about 30 seconds, not allowing them to splash onto the lid or over the edge. The media (or liquid agar) was observed to solidify after cooling and is more opaque than the yellowish liquid media prepared. After solidification, the plates were inverted to prevent moisture from condensing on the surface. The 3 plates of solidified agar were then incubated at 37℃ for 24 hours to form visible cell colony. The test tubes were washed and allowed to dry to be used the next day.

2.3.5 Colony Counting

On day 2, the plates were removed from the incubator and colonies counted using the CC-J3 colony counter and results recorded for SDE1, SDE2 & SDE3. CFU/ml was then calculated using Equation 4 (Arana et al., 2013; Um-e-Habiba et al., 2021).

$$\text{CFU/ml} = \frac{(\text{No. of colonies})(\text{Total dilution factor, TDF})}{\text{Volume of culture plated in mL}} \quad (4)$$

Using TDF = 10^9 for 1ml of inoculum plated, CFU/ml of the triplicate step were recorded. The average of these data were then computed as initial microbial concentration of day 1 (X_0) of the CM feedstock. The used plates were then discarded. The method was carried out according to explanations given by Brugger et al. (2012).

To ensure homogeneous composition of substrate, expedite cell growth and break possible agglutination of bacterial cells in the digester, the mixed CM slurry was stirred using the manual stirrer before taking the 5ml sample for microbial count. For subsequent days, microbial concentration, X, was determined repeating the serial dilution, pour plating and colonic counting procedures. Specifically, out of the 500ml of NA prepared, 3×20ml = 60ml was used a day and 480 ml in 8 days before another culture media was prepared. When X starts to decrease, the death phase of the bacteria is therefore reached and cell counts stops. The bacterial concentrations recorded over these periods was recorded as $X_{Expt.}$ implying cell concentration gotten from the SDEs for the triplicate run of experiment.

2.4 Growth Kinetics

In cell growth kinetics, growth infer cell replication plus a change in cell size. To keep growing, cells need to take nutrients from the CM slurry and change them to cellular matter (biomass) and energy (Harahap et al., 2023). It is an autocatalytic process described by Equation 5 and 6.

$$\text{Substrate/nutrient} + \text{cells/biomass} \rightarrow \text{extracellular products} + \text{more cells} \quad (5)$$

$$\sum_i S_i + X \rightarrow \sum_j P_j + nX, \qquad n > 1 \quad (6)$$

Relationship between S, X, product (P) and associated models was used to study the kinetics of biogas production from CM.

2.4.1 Growth Curve Plot

To depict the microbial growth curve for the CM slurry containing microbes, the logarithm of the average cell concentration ($X_{avg.}$) from the 3 SDEs was taken. A plot of this logarithm versus time always gives the growth curve and was used to explain the different phases of the microbial growth and the resulting biogas output.

2.4.2 Finding Generation Time and Decay Constant

To find the generation time, G at the exponential growth phase of the microorganisms, Equation (7) presented by Maier (2009) was linearized to give Equation (8) as $G = \frac{t}{n}$,

$$N = N_0 2^n \quad (7)$$

$$\log N = \log N_0 + \frac{t}{G}\log 2 \quad (8)$$

Where, t = interval of time, N_0 = initial number of cells, and N = number of cell after a certain time. At the death phase, the rate of cell death also given by Maier was determined according to Equation (9),

$$\frac{dX}{dt} = -bX \quad (9)$$

Where, X = cell concentration (mg/l), b = decay constant (hr-1) and t = retention time (hr). Equation 9 was integrated over the initial ($X_{D,0}$) and final cell concentration (X_D) within the death period to give Equation 10.

$$X_D = X_{D,0} e^{-bt} \quad (10)$$

Equation 11 was then used to estimate the first-order decay coefficient or kinetic constant of the death occurrences, b.

$$\ln(X_D) = \ln(X_{D,0}) - bt \quad (11)$$

Appropriately, $X_{D,0}$ = number of cells (concentration) in the medium at the end of the stationary phase while X_D = number of cells at time t into the death phase. Using Equation (11), a plot of $\ln(X_D)$ versus time was made and 'b' was calculated from the slope of the graph.

2.4.3 Substrate Utilization Model

The notion that organisms consume substrate in 3 ways was used to formulate relationships for the rate of substrate utilization, $\left(-\frac{dS}{dt}\right)$ as given in Equation 12 according to Yang et al. (2021).

$$-\Delta S = \left(-\frac{dS}{dt}\Big|_{maintenance}\right) + \left(-\frac{dS}{dt}\Big|_{cells}\right) + \left(-\frac{dS}{dt}\Big|_{product}\right) \quad (12)$$

Equation 12 was reduced to Equation 13 by assuming that multiple substrate are present to aid cell maintenance, hence there is rapid depletion of substrate to zero, so that $-\frac{dS}{dt}\Big|_{maintenance} = 0$ and no chemical product is formed so that $-\frac{dS}{dt}\Big|_{product} = 0$. Rate of substrate disappearance was estimated using Equation 13 (Syaichurrozi & Rusdi, 2020), where q is the specific substrate utilization rate ($m_{substrate}/m_{cells.time}$), and K_h is the first order hydrolysis constant.

$$-\frac{dS}{dt} = \frac{1}{Y_{X/S}}\frac{dX}{dt} = \frac{\mu X}{Y_{X/S}} = qX = K_h S \quad (13)$$

Making S subject in Equation 2, S data was generated via Equation 14 and is termed S-experimented or $S_{Expt.}$.

$$S_{Expt.} = S_o - \frac{X_{Expt.} - X_o}{Y_{X/S}} \quad (14)$$

2.4.4 Material Balance

For the well-mixed unsteady state batch biological system (Figure 1) where all nutrients are fed initially into the culture and cells produced in the culture grow until one or more nutrient is exhausted, material balance over this process was formed as shown in Equation 15-19.

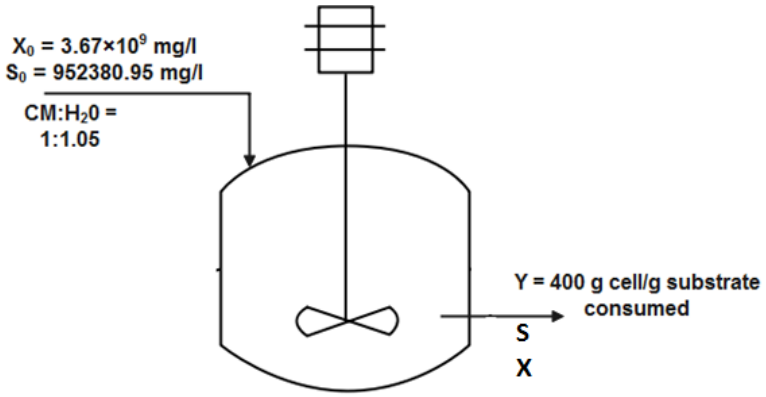

Figure 1: Flow Diagram of the Batch System

Overall balance: Accumulation = Input – Output + Generation (15)

Cells: $\frac{d(VX)}{dt} = F_{in}X_{in} - F_{out}X_{out} + r_x V$ (16)

Limiting substrate: $\frac{d(VS)}{dt} = F_{in}S_{in} - F_{out}S_{out} + r_s V$ (17)

Product: $\frac{d(VP)}{dt} = F_{in}P_{in} - F_{out}P_{out} + r_p V$ (18)

Water: $\frac{d(VW)}{dt} = F_{in}W_{in} - F_{out}W_{out} + r_w V$ (19)

Subscript 'in' and 'out' implies input and output respectively, where F = flow rate, r = rate, S = substrate, X = cell, W = water and P = product. A batch process is a closed culture occurring when $F_{in} = F_{out} = 0$ and volume, V is constant. The ideology was implemented for other possible assumptions which are (a) concentration of H_2O remains the same ($W_{in} = W_{out}$) and insignificant water is generated (r_w), (b) reactor is well-mixed ($P_{out} = P_{in}$; $S_{out} = S_{in}$; $X_{out} = X_{in}$), (c) no product in feed ($P_{in} = 0$) and (d) cell growth is greater than cell death rate ($r_x = \mu X$) to give Equations 20 and 21.

Cells: $\frac{dX}{dt} = \mu X = r_x$ (20)

Substrate: $\frac{dS}{dt} = r_s$ (21)

2.5 Generating Appropriate Data for Monod Plot

Monod Equation given in Equation 22 (Um-e-Habiba et al., 2021)(Mitra & Dutta, 2018) was used to prove the fact that a relationship exists between S and μ.

$\mu = \frac{\mu_{max} S}{K_s + S}$ (22)

Specific growth rate, μ, can be positive (growth) or negative (death) and is a function of pH, temperature, osmotic pressure and concentration of inhibitors, product and substrate. Most importantly, calculated values of new X and S data, X_{calc} and S_{calc} was obtained by regression through estimation of two parameters, K_s and μ_{max} necessary for optimization of the process via the listed steps. b

Step 1 – the carrying capacity of the environment or maximal biomass concentration, X_∞ was calculated using Equation 23 given by Mitra & Dutta (2018).

$X_\infty = X_0 + YS_0$ (23)

Mitra & Dutta (2018) also provides Equation 24, used independently for estimating μ without Monod, which was combined with Equation 20 (see Equation 25) and integrated to give Equation 26.

$\mu = k\left(1 - \frac{X}{X_\infty}\right)$ (24)

$\frac{dX}{dt} = \mu X = k\left(1 - \frac{X}{X_\infty}\right)X$ (25)

$X_{calc} = \frac{X_0 e^{kt}}{1 - \frac{X_0}{X_\infty}[1 - e^{kt}]}$ (26)

Regression was performed using POLYMATH 6.10 Educational Release software to find new data that fits $X_{Expt.}$ versus time (hr) called X_{calc}, thereby estimating the k value. S_{calc} was thus, computed using Equation 27.

$S_{calc} = S_o - \frac{X_{calc} - X_o}{Y_{X/S}}$ (27)

Step 2 – By combining Monod (Equation 22) and Equation 24, as Equation 28, X_{calc} data was used to determine K_s by finding new set of S data (or S_{reg}) that fits S_{calc} data using POLYMATH.

$$S_{reg} = \frac{K_S\left(\frac{X_\infty - X_{calc}}{X_\infty}\right)}{\frac{\mu_{max}}{k} - \left(\frac{X_\infty - X_{calc}}{X_\infty}\right)} = \frac{K_S\left(\frac{X_\infty - X_{calc}}{X_\infty}\right)}{Y - \left(\frac{X_\infty - X_{calc}}{X_\infty}\right)} \quad (28)$$

Both X_{calc} and S_{calc} as well as $X_{Expt.}$ and $S_{Expt.}$ values were plotted against time and graphs were compared.

Step 3 – Rate of biomass growth, $\frac{dX}{dt}$, was estimated using X_{calc} data by substituting into Equation 25 with known k. From Equation 24, μ was estimated using Equation 29 (Um-e-Habiba et al., 2021).

$$\mu = \frac{1}{X_{calc}}\frac{dX}{dt} \quad (29)$$

Step 4 – Equation 22 and 24 was combined knowing that $\mu_{max} = k$ so as to customize and compute S values now called S_{Monod} given by Equation 30.

$$S_{Monod} = \frac{K_S}{X_{calc}}(X_\infty - X_{calc}) = \frac{\mu K_S}{\mu_{max} - \mu} \quad (30)$$

Step 5 - μ in step 3 and S_{Monod} in step 4 was plotted to give the Monod plot, selecting only values from the growth phase, as the Monod equation is only valid at the exponential phase. From the Monod plot, μ_{max} and K_s was further confirmed. Rate of substrate utilization, r_s or $(\frac{dS}{dt})$ as well as that of cell production, r_x or $(\frac{dX}{dt})$ was determined using Equation (13 or 21) and (20 or 25) respectively.

3. Results and Discussion

3.1 Effect of CM Characteristic

The following results including MC = 47%, TS = 53%, AC (wet basis) = 22.6%, OM = 88%, PD = 0.0163 g/cm^3, C/N ratio = 24:1 and VS = 13.21% were obtained in 5g of CM sample used before digestion. It is important to have considerable amount of moisture and a low PD in the CM, that will be able to harbor microorganism in the feedstock, as feedstock with PD>1 means the specimen is not porous enough for the bacteria to break down the substrate as indicated by Brunerová et al. (2020). A completely dry CM speculates the presence of less OM and a microorganism-free feedstock making CM utilization for product generation impossible. Therefore %TS and MC around the 50:50 range is most likely to give the desired result. The C/N ratio of 24:1 will generate less volatile fatty acid responsible for pH fluctuation in the feedstock as most microorganism do not grow in acidic environment, except the lactic acid bacteria which is rarely found in CM. A low VS content compared to %TS obtained in this work means there is more of the solid material containing nutrients than solids that would have disappear before charging into the digester.

3.2 Analysis of Growth Kinetics

Microbial concentration (CFU/ml) of the triplicate SDE is shown in Figure 2(a-c). The SDEs provides almost identical plot as shown in Figure 2(d), a further demonstration of accuracy of results. It is further attributed to high TDF which enable bacterial colonies to be seen and counted. If TDF is low, colonies would be Too Numerous to Count (TNTC). Colonies > 300 are considered TNTC (Andr & Parker, 2020; Sieuwerts et al., 2008) and would make generation of data for kinetic study very difficult. Despite the colonies are an average of 48 colonies > 300, after incubation (maximum number of colonies for SDE1 = 350, SDE2 = 346 and SDE3 = 348, producing an average of 343 colonies beyond the theoretical counting limits at t = 30-37 days). Though difficult, other authors had reported

colonies above 300 for kinetic study. Colonies that are < 30 or Too Few to Count (TFTC) are not preferred (Sieuwerts et al., 2008), it is however very significant in this study. Few colonies were counted for 13 days as shown in Figure 4 of the log-log plot of the average cell concentration.

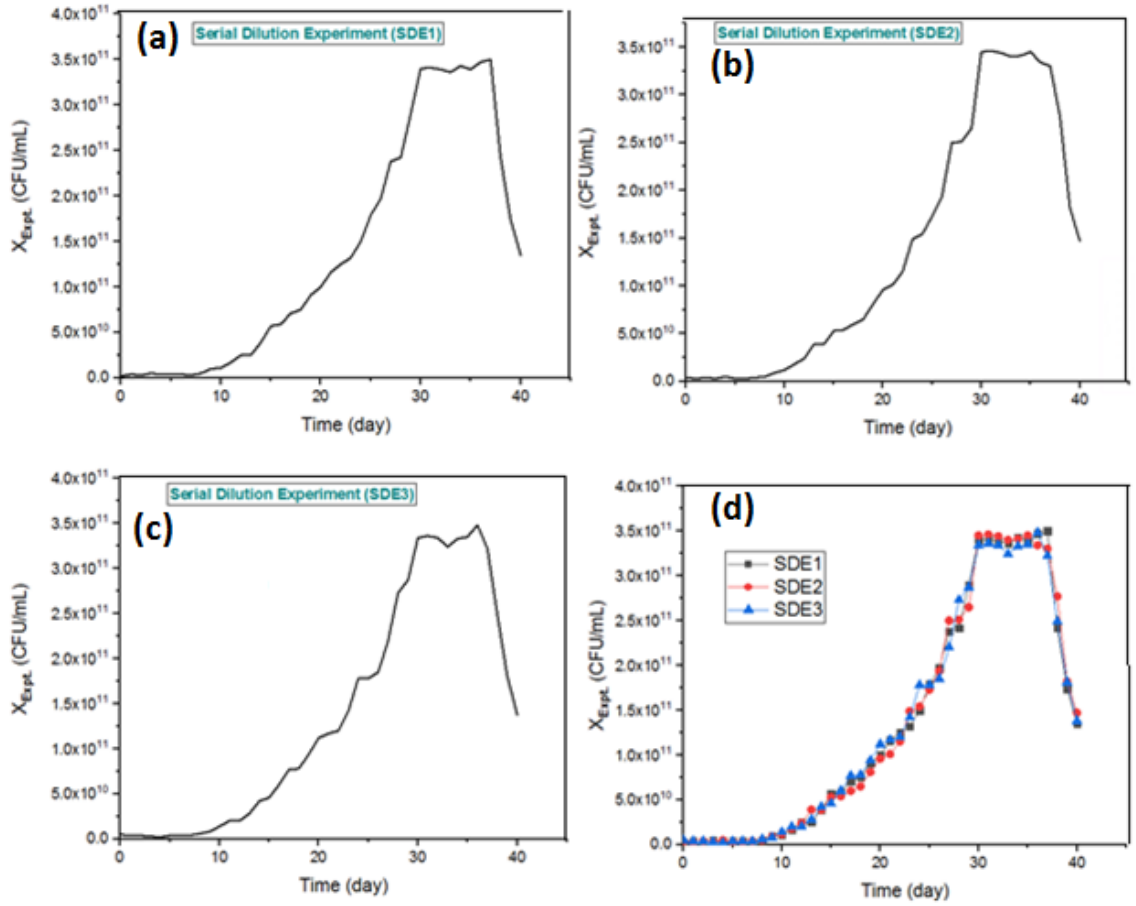

Figure 2: Cell Concentration against Time for the SDEs

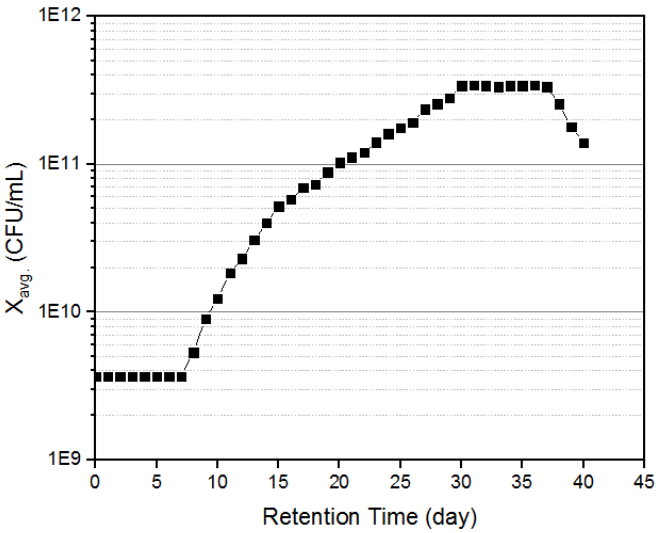

Figure 4: Average Cell Concentration Versus Time on a Log-log Scale

From an initial bacterial concentration, X_0=3.67× 〖10〗 ^9CFU/ml at t = 0 day maintained for 7 days, concentration increases exponential to X = 3.40× 〖10〗 ^11CFU/ml at t = 23 days, maintaining an average value of X = 3.38× 〖10〗 ^11CFU/ml for 7 days and falling to X = 1.40× 〖10〗 ^11CFU/ml. These change in X pattern forms the growth curve. It could be assumed that biogas formation decreases to almost zero when the bacteria in

the feedstock begin to die. Here, the bacterial cells in the CM slurry after counting was observed to decrease from X = 3.34× 〖10〗 ^8 mg/l on day 37 to X = 2.56× 〖10〗 ^8 mg/l on day 38, maintaining this downward trend to the 40th day and brings to an end the task of counting the cells. Biogas production increased accordingly with the trend seen in Figure 4, from an initial volume of 8.3× 〖10〗 ^(-4) m3 to a final volume of 0.883 m3 which is less than the volume from 20kg of cow dung and 10kg of domestic waste as reported by Jyothilakshmi & Prakash (2016). However, the approximately 1 m3 of biogas generated using 7 kg of CM, falls in the range of 0.065-0.116m3 obtained from chicken dung anaerobic digestion in Neupane (2018).

3.3 Discussion on Bacterial Growth Phases

Origin of microbial presence in CM is the chicken intestine (commonly, Firmicutes & Proteobacteria) which continue to survive even after its being excreted (Lam et al., 2022), and grows if kept in an environment similar to a bioreactor. Logarithm of the average cell concentration plotted against fermentation time is shown in Figure 5, where the four significant phases of cell growth is illustrated.

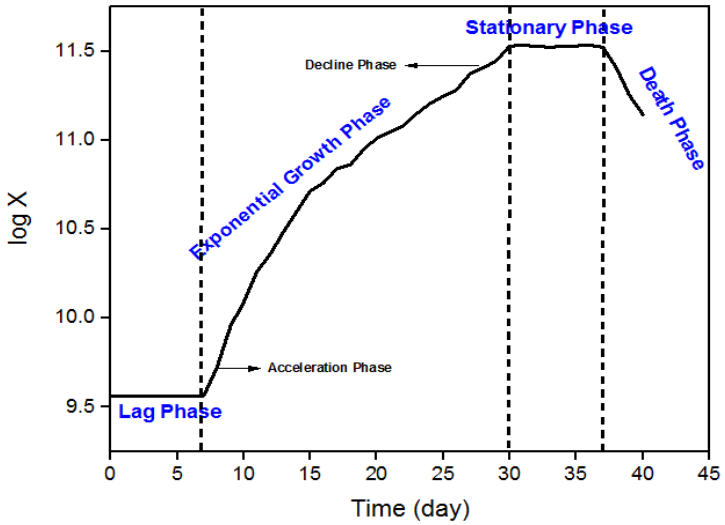

Figure 5: Microbial Growth Curve

The plot is identical to Figure 4, depicting the lag phase where bacteria acclimatize by synthesizing necessary enzymes to degrade substrate and other biochemicals. That is, rate of cell accumulation, $\frac{dX}{dt} = 0$. The growth phase is where rate of growth > rate of death, which follows the equation for exponential growth given by $\frac{dX}{dt} = \mu X$. At this point gas production increases rapidly. The population begins to decline to a point where rate of growth is equivalent to the rate of death or $\frac{dX}{dt} = 0$. Death phase is caused by cell destruction and decomposition and is usually a short period of time observed in minimal increase in biogas generation. At the acceleration phase, available cells $N_0 = 3.67$ with concentrations $X_0 = 3.67 \times 10^6$mg/l, begin to multiply by continuously forming duplicates. The slight curving of the supposed linear plot in Figure 5 and 6 might be linked to superimposed growth rates of the respective bacteria inside the CM. From the phase through the growth phase to the final decline phase, Figure 6 where the generation time (G) can be estimated was plotted using data in the region along the growth phase to the final decline phase.

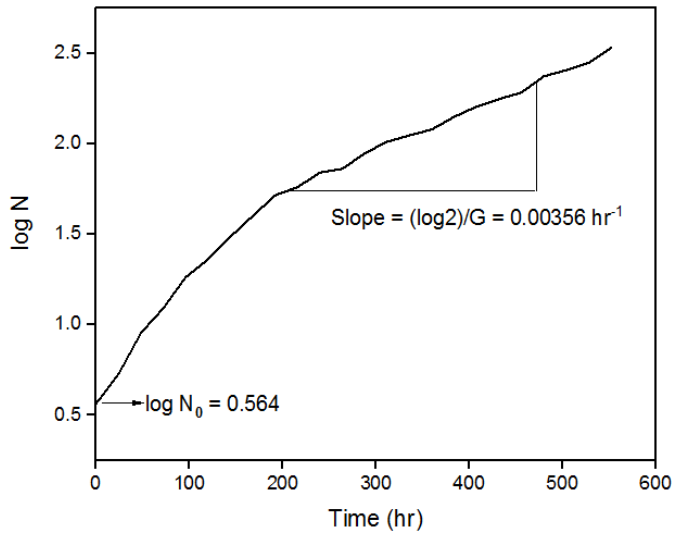

Figure 6: Biomass Doubling Time Estimation

Hence, G = 84.56 hours cannot be compared with literature works that mostly reports G for specific bacteria inside their substrate. For example Gibson et al. (2018) found that under aerobic and nutrient-rich condition, bacterium such as *Escherichia coli* can divide every 20 min in the laboratory while *Salmonella enterica*, divides every 0.5 hour. He also affirmed that the doubling time of most bacteria in their natural environment is not known, which is why majority of reported data in the literature are for simulated environment provided for the bacteria. At the death phase, where $\frac{dX}{dt} = -bX$, first order decay constant or the kinetic constant of death occurrences 'b' was determined from Figure 7 as b = $-0.0006hr^{-1}$.

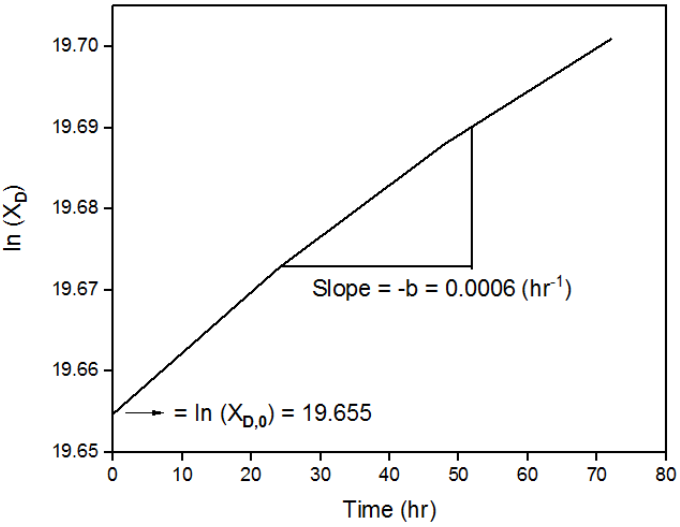

Figure 7: Determination of Death Constant

Figures 8 and 9 shows that as bacteria population increases, substrate concentration decreases. Predicted data plot in Figure 9b fits properly to the experimental results and hence estimates the parameters k = 0.07316 hr^{-1} and $K_s = 3.838 \times 10^8$ mg/l correctly. Figure 8a also shows the behavior of the CM substrate concentration through the various phases of the growth of microorganism, which was initially high at $S_0 = 952380.95$ mg/l and decreased to an average constant value (S = 115476.1881 mg/l) at the stationary phase. At the end of the stationary phase, only few bacteria were alive to further decompose the feedstock and hence reduce the substrate concentration. Concentration of the substrate at the death phase is the remaining amount in the reactor and might increase slightly due to added weight of the dead bacteria.

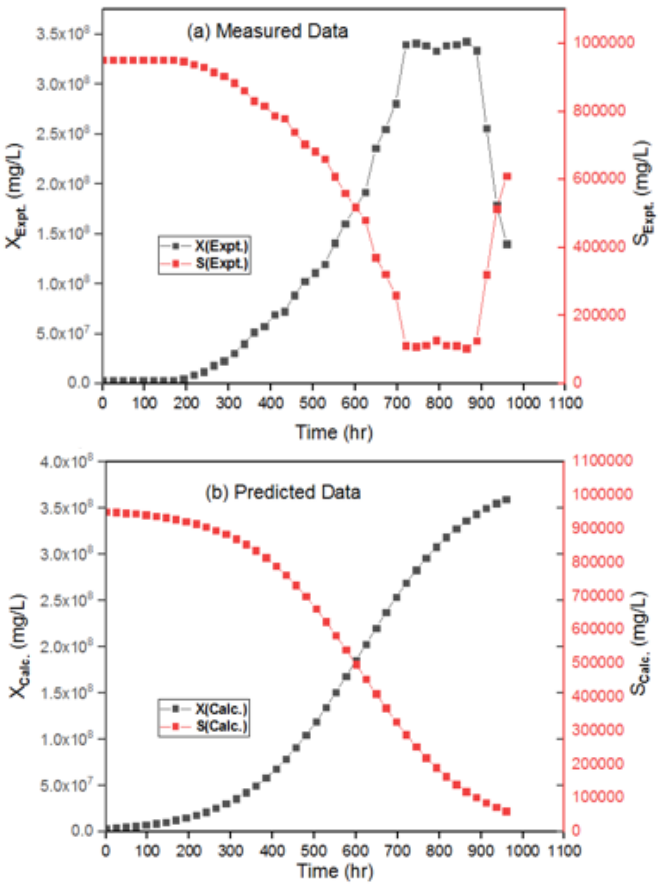

Figure 8: Substrate and Biomass Concentration from SDE and Kinetic Equation

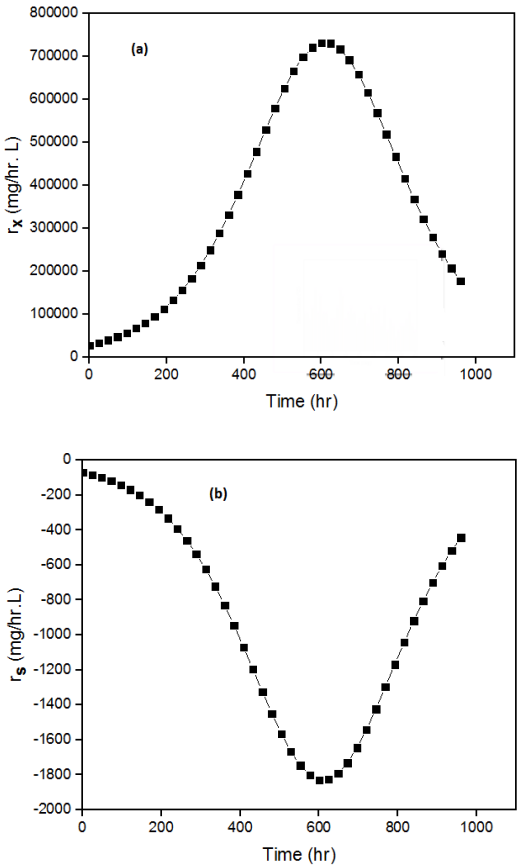

Figure 9: (a) Rate of Cell Growth (b) Rate of Substrate Consumption

Plots obtained in Figure 8b is the characteristic plots usually obtained from such experiment – as batch degradation of phenol by indigenous monoculture of Pseudomonas aeruginosa carried out by Agarry et al. (2010) follows similar trend. It is also clear that plots of cell and substrate behaviour as seen in Figure 9 can be replicated using Equation 26 and 27 taken from material balance carried out earlier, so as to obtain rates of their respective changes with time. Linear relationship between the substrate concentration and the cell concentration exist. Figure 10 better explains this relationship looking at it from the bottom right upwards (where X is high and S is low).

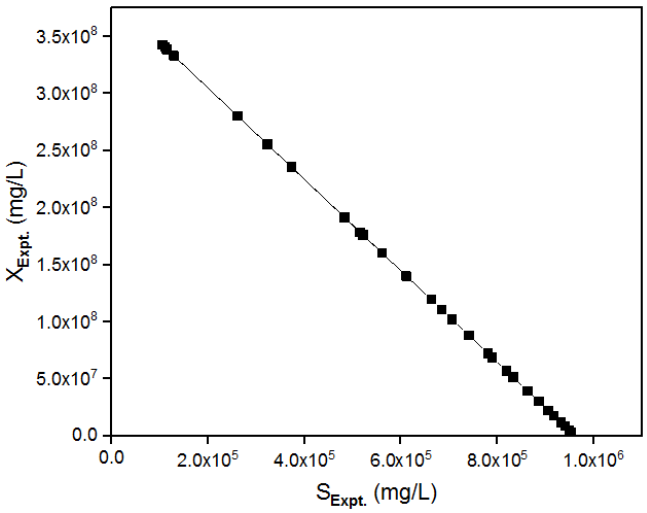

Figure 10: Showing the Relationship between Substrate Concentration and Cell Concentration

Accuracy in bacterial population count is very difficult, though this data assumes that single bacteria grows to form a single colony, multiple bacteria forming single colony hides some number of viable cells that were unknowingly counted as one. Values of X therefore doesn't guarantee a 100% precise data because it fails to include gain in concentration due to growth in weight/size of the bacteria. Against the typical mass of bacteria which is 1pg, bacteria inside the slurry are capable of growing to 1ng or their sizes might be even less (e.g., 1fg). However, assuming a weight of 1ng in this work wouldn't pose much problem to kinetic analysis. Despite this, plot as the one shown in Figure 10 must depict ideal conditions of X and S as explained earlier.

3.4 Effect of Substrate Concentration on Specific Growth Rate

The rectangular hyperbola in Figure 11 is called the Monod plot based on cell growth at the exponential phase.

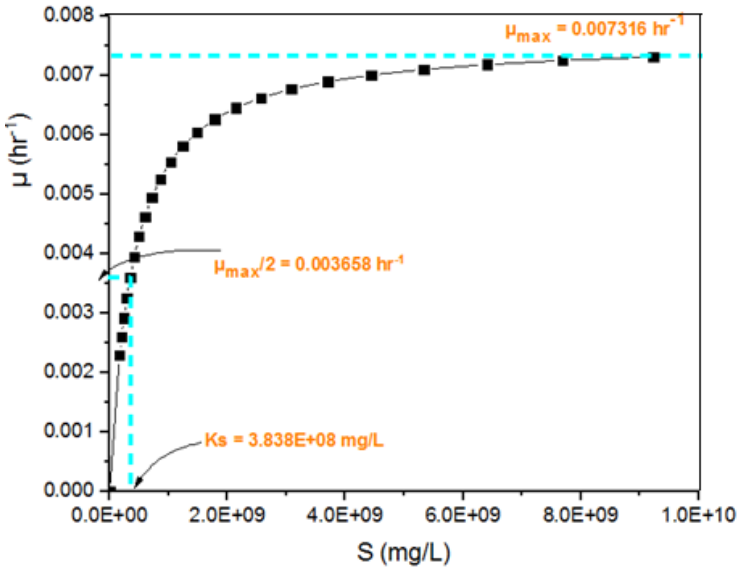

Figure 11: Monod Plot Based on μ and S Computed from Experimental Values of Microbial Concentration

It starts from S = 0 mg/l corresponding to $\mu = 0\ hr^{-1}$, to a peak value, μ_{max} where S is also high. The plot is divided into 3-sections based on S amount. For low S (i.e. $S \ll K_s$), growth have first order dependence on S (growth is highly sensitive to S) and the Monod equation reduces to $\mu = \frac{\mu_{max} S}{K_s}$. That is, when S (nutrient) is very little, cells had to compete for it.

This points to the fact that amount of substrate limits how fast the cells can grow. So, addition of more substrate causes proportional increase in cell growth rate. The center region is called the mixed order section that satisfies the Monod equation proper. When S is high (i.e. $S \gg K_s$), growth is at μ_{max} and kinetics reduces to a zero-order expression $\mu = \mu_{max}$. Here, each cell can have as much nutrient or substrate as they so desire due to its abundance because the specific growth rate is high and constant. The explanation of the substrate relationship with the saturation constant was earlier explained by Maier and is in accordance with the present study. Figures 11 and 12 are intruments for determining μ_{max} and K_s.

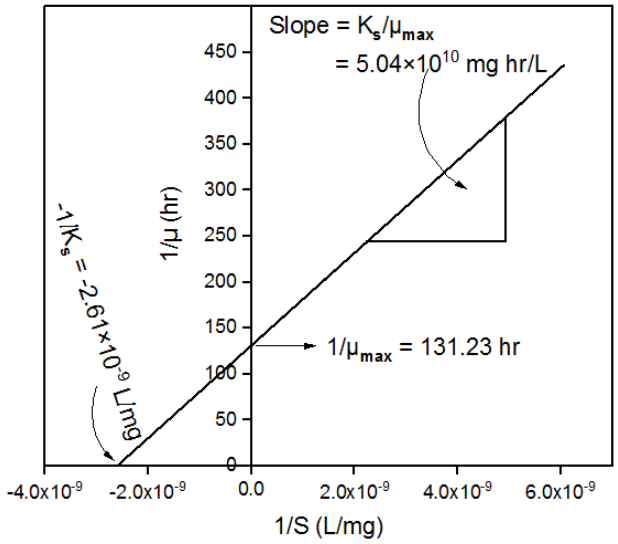

(a) Line weaver-Burke Plot

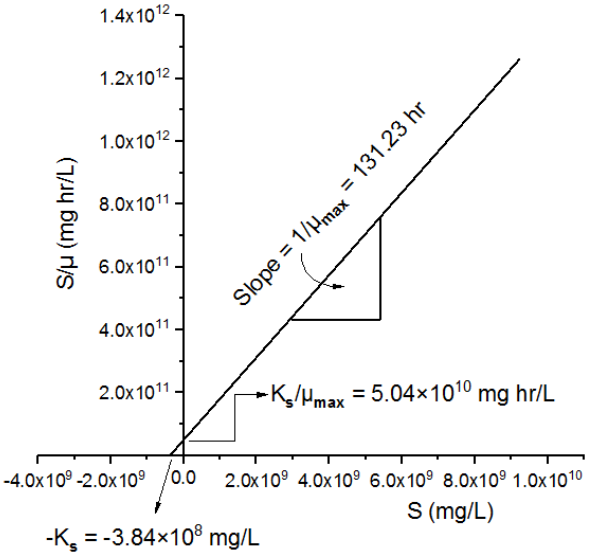

(b) Hanes-Woolf Plot

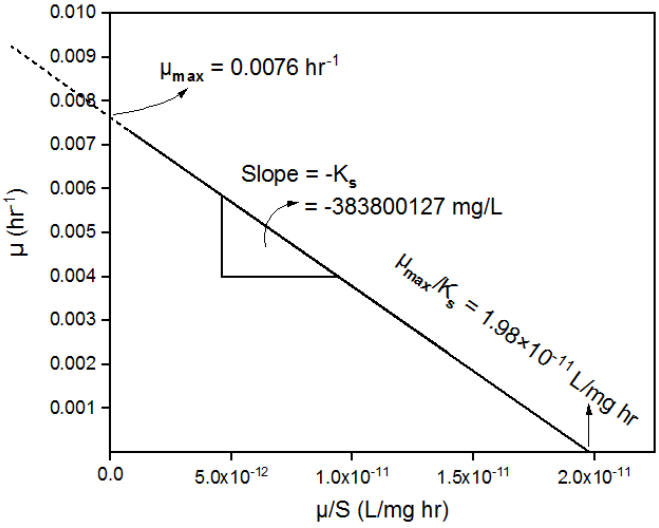

(c) Eadie-Hofstee Plot

Figure 12: Alternative Plot for Determining Monod Parameter

The S data used for estimating these parameters excludes toxic S that are capable of inhibiting bacteria growth. For example, high concentration (300 mg/L) of tetracycline antibiotics inhibits anaerobic digestion of microorganisms, in accordance with the study conducted by Zhai & Qiang (2022). The two parameters (μ_{max} and K_S) estimated earlier, can be determined alternatively using Lineweaver-Burke plot, Hanes-Woolf pot or Eadie-Hofstee plot (all linear). Equations for these plots were derived from actual Monod equation and provides a much easier approach of estimating the Monod kinetic parameters, as already seen in Figure 12. Equations of the respective Lineweaver-Burke Plot, Hanes-Woolf Plot and the Eadie-Hofstee Plots for results obtained here are given in Equations 31-33.

$$\frac{1}{\mu} = \frac{3.838\times10^{8}}{0.007316}\left(\frac{1}{S}\right) + \frac{1}{0.007316} \quad (31)$$

$$\frac{S}{\mu} = \frac{3.838\times10^{8}}{0.007316} + \frac{1}{0.007316}S \quad (32)$$

$$\mu = 0.007316 - 3.838\times10^{8}\frac{\mu}{S} \quad (33)$$

The above model equations can hence be used for S and μ estimates spanning the period of the experimental growth phase. Abubakar et al. (2017) demonstrate the use of

Lineweaver-Burke plot to estimate μ_{max} and K_s from their experimental result. But the equation; G or $t_d = \ln\frac{2}{\mu}$ given by the same author needs to be checked or verified for possible use because it is different compared to the normally reported one to compute the doubling time.

Successful anaerobic digestion of CM would not only be a means of manufacturing biogas in high quantity, but also a reliable source for the production of the intermediate product of anaerobic digestion called volatile fatty acids (Yin et al., 2022). Zeolite can be added to adsorb ammonia from CM leachate during anaerobic digestion to improve its biochemical methane potential (Spyridonidis et al., 2022). Interestingly, other derivative by-product of chicken waste like chicken eggshell contains micro- and macro-nutrients microorganisms could feed on to generate biogas or bio-resource (Ajala et al., 2018). Experiments shows that biogas could serve as a modern resource for keeping poultry houses warm; having the advantage of small-scale production to serve that purpose (Ebrahem et al., 2022; Wahidah et al., 2022).

4. Conclusion

Microbial growth kinetics of biogas production using CM and that CM mixed with other additives or organic matter differs in terms of performance variables estimated (for the CM sample) from any existing growth model, due to several factors that may alter microbial growth pattern or the quantity of gas generated. Multiple microorganisms inside CM feedstock affects the growth period observable during experiment. So, in this work, all microorganism present were treated as one, though the dissimilarity was seen in plots of the generation time. Despite this, natural trend followed by plots of substrate concentration which is 9.5×10^5 mg/l in this work against cell concentration obtained from triplicate SDEs is not visibly affected. It is clear that the two concentrations are inversely related with few or plentiful of nutrients, as well as right pH and temperature which gives a good Monod plot.

Authors Contribution
Abdulhalim Musa Abubakar: literature search, write up
Kiman Silas: study design and concept, write up
Mohammed Modu Aji: data collection, write up
Usman H. Taura: analysis, write up
Jerome Undiandeye: critical revision and incorporation of intellectual content, write up

Conflict of Interests/Disclosures
The authors declared no potential conflicts of interest w.r.t the research, authorship and/or publication of this article.

References

Abubakar, B. S. U., Abdullah, N., Idris, A., Zakaria, M. P., & Shokur, M. Y. (2017). Estimating the biodegradation kinetics by mixed culture degrading pyrene(pyr). In *Arid Zone Journal of Engineering, Technology and Environment* (Vol. 13, Issue 1). www.azojete.com.ng

Agarry, S. E., Solomon, B. O., & Audu, T. O. K. (2010). Substrate utilization and inhibition kinetics: Batch degradation of phenol by indigenous monoculture of Pseudomonas aeruginosa. *International Journal for Biotechnology and Molecular Biology Research*, *1*(2), 22–30. http://www.academicjournals.org/IJBMBR ISSN

Ajala, E. O., Eletta, O. A. A., Ajala, M. A., & Oyeniyi, S. (2018). Characterization and evaluation of chicken eggshell for use as a bio-resource. *Arid Zone Journal of Engineering, Technology and Environment (AZOJETE)*, *14*(1), 26–40. www.azojete.com.ng

Alskory, M. A. M., Hamad, T. A. M., Hamad, Y., & Alhasee, F. M. S. (2021). Improving the amount of biogas production from cow manure by adding chicken manure via

anaerobic digestion. *ICRSE 2021: The 1st International Conference on Renewable and Sustainable Energy*, 150–154.

Andr, J., & Parker, A. E. (2020). *Systematic statistical analysis of microbial data from dilution series*.

Arana, I., Orruno, M., & Barcina, I. (2013). *How to solve practical aspects of microbiology* (pp. 1–10).

Brugger, S. D., Baumberger, C., Jost, M., Jenni, W., Brugger, U., & Muhlemann, K. (2012). Automated counting of bacterial colony forming units on agar plates. *PLOS ONE*, *7*(3), 1–6. https://doi.org/10.1371/journal.pone.0033695

Brunerová, A., Müller, M., Gürdil, A. G. K., Sleger, V., & Brozek, M. (2020). Analysis of the physical-mechanical properties of a pelleted chicken litter organic fertiliser. *Research in Agricultural Engineering*, *66*(4), 131–139. https://doi.org/10.4491/eer.2018.081

Buivydas, E., Navickas, K., Venslauskas, K., Zalys, B., Zuperka, V., & Rubezius, M. (2022). Biogas production enhancement through chicken manure co-digestion with pig fat. *Applied Sciencesiences*, *12*(4652), 1–17. https://doi.org/10.3390/app12094652

Cahyono, N. A. D., Shamsuddin, R., Ayoub, M., Siyal, A. A., & Hamid, A. F. (2023). Anaerobic co-digestion of chicken manure with sugarcane bagasse, oil palm frond and empty fruit bunch additive: Methane yield and kinetic analysis. *Bioresource Technology Reports*, 1–18.

Ebrahem, M. E., Moustafa, M. M., & Abdel-Salam, M. F. (2022). Biogas utilization system for warming poultry houses. *MISR Journal of Agricultural Engineering (MJAE)*, *39*(2), 341–352. https://doi.org/10.21608/mjae.2022.122971.1066

Gallipoli, A., Braguglia, C. M., Gianico, A., Montecchio, D., & Pagliaccia, P. (2020). Kitchen waste valorization through a mild-temperature pretreatment to enhance biogas production and fermentability: Kinetics study in mesophilic and thermophilic regime. *Journal of Environmental Sciences*, *89*, 167–179. https://doi.org/10.1016/j.jes.2019.10.016

Gibson, B., Wilson, D. J., Feil, E., & Eyre-walker, A. (2018). *The distribution of bacterial doubling times in the wild* (Vol. 285). Royal Society Publishing. https://doi.org/10.1098/rspb.2018.0789

González-figueredo, C., Flores-estrella, R. A., & Rojas-rejón, O. A. (2018). Fermentation: Metabolism, kinetic models, and bioprocessing. In *Current Topics in Biochemical Engineering* (pp. 1–17). InTech Open. https://doi.org/10.5772/intechopen.82195 solid

Haleem, A. M., Al-bakri, S. A., & Al-Hiyaly, S. A. K. (2013). Determination of microbial content in poultry meat in local Iraqi markets. *Journal of Microbiology Research*, *3*(6), 205–207. https://doi.org/10.5923/j.microbiology.20130306.02

Harahap, D. E., Wahyuni, S. H., Darwis, M., Harahap, M. F., & Maulana, M. (2023). Analysis of macro nutrients of chicken manure decomposed Bytrichoderma viridemushrooms with different storage lengths. *International Journal of Science and Environment*, 30–33. https://ijsenet.com

Hawkins, J. L., Uknalis, J., Oscar, T. P., Schwarz, J. G., Vimini, B., & Parveen, S. (2019). The effect of previous life cycle phase on the growth kinetics, morphology, and antibiotic resistance of Salmonella Typhimurium DT104 in brain heart infusion and ground chicken extract. *Frontiers in Microbiology*, *10*(1043), 1–11. https://doi.org/10.3389/fmicb.2019.01043

Hurst, G., Ruiz-Lopez, S., Rivett, D., & Tedesco, S. (2022). Effect of hydrochar from acid hydrolysis on anaerobic digestion of chicken manure. *Journal of Environmental Chemical Engineering (JECE)*, 1–39. https://doi.org/10.1016/j.jece.2022.108343

Jaman, K., Amir, N., Musa, M. A., Zainal, A., Yahya, L., Malek, A., Wahab, A., Suhartini, S., Nurfarhana, T., Mohd, T., Harun, R., & Idrus, S. (2022). Anaerobic digestion, codigestion of food waste, and chicken dung: Correlation of kinetic parameters with digester performance and on-farm electrical energy Generation Potential. *Fermentation*, *8*(28), 1–19. https://doi.org/10.3390/fermentation8010028

Johari, S. A. M., Aqsha, A., Shamsuddin, R., Lam, M. K., Osman, N., & Tijani, M. (2023). Technical trends in biogas production from chicken manure. In M. Jawaid & A. Khan (Eds.), *Manure Technology and Sustainable Development* (pp. 145–182). https://doi.org/10.1007/978-981-19-4120-7_6

Jyothilakshmi, R., & Prakash, S. V. (2016). Design, fabrication and experimentation of a

small scale anaerobic biodigester for domestic biodegradable solid waste with energy recovery and sizing calculations. *Procedia Environmental Sciences*, *35*, 749–755. https://doi.org/10.1016/j.proenv.2016.07.085

Kalogiannis, A., Vasiliadou, I. A., Spyridonidis, A., Diamantis, V., & Stamatelatou, K. (2022). Biogas production from chicken manure wastes using an LBR-CSTR two-stage system: Process efficiency, economic feasibility, and carbon dioxide footprint. *Journal of Chmeical Technology and Biotechnology*, 1–10. https://doi.org/10.1002/jctb.7170

Ksheem, A. M. A. (2015). *Optimising nutrient extraction from chicken manure and compost* [University of Southern Queensland]. https://doi.org/10.13140/RG.2.1.1973.3842

Lam, T.-K., Yu, C.-P., & Wu, S.-H. (2022). Metagenomics analysis on the microbiota of chicken manure anaerobic digestion materials in biogas production. *Research Square*, 1–23. https://doi.org/10.21203/rs.3.rs-2197661/v1

Maier, R. M. (2009). Bacterial growth. In *Review of Basic Microbiological Concepts* (pp. 37–54). Academic Press Inc.

Manogaran, M. D., Shamsuddin, R., Yusoff, M. H. M., Lay, M., & Siyal, A. A. (2022). A review on treatment processes of chicken manure. *Cleaner and Circular Bioeconomy*, *2*(100013), 1–11. https://doi.org/10.1016/j.clcb.2022.100013

Matheri, A. N., Ndiweni, S. N., Belaid, M., Muzenda, E., & Hubert, R. (2017). Optimising biogas production from anaerobic co-digestion of chicken manure and organic fraction of municipal solid waste. *Renewable and Sustainable Energy Reviews*, *80*, 756–764. https://doi.org/10.1016/j.rser.2017.05.068

Mitra, R., & Dutta, D. (2018). Growth profiling, kinetics and substrate utilization of low-cost dairy waste for production of β -cryptoxanthin by Kocuria marina DAGII. *Royal Society Open Science*, *5*(172318), 1–19. https://doi.org/10.1098/rsos.172318

Muloiwa, M., Nyende-byakika, S., & Dinka, M. (2020). Comparison of unstructured kinetic bacterial growth models. *South African Journal of Chemical Engineering*, *33*, 141–150. https://doi.org/10.1016/j.sajce.2020.07.006

Najafi, B., Ardabili, S. F., Shamshirband, S., & Chau, K. (2019). Development of a modified kinetic method for modelling of biogas produced from biomass. *Energies*, 1–16.

Nauanova, A., Yerpasheva, D., Shakhabayeva, G., Yermekov, A., & Baimbetova, E. (2020). Identification and screening of microorganisms common in poultry manure. *Systemic Review in Pharmacy*, *11*(12), 1582–1588.

Neupane, S. K. (2018). Biogas production from poultry faeces. *Innovative Energy & Research*, *7*(4), 1–6. https://doi.org/10.4172/2576-1463.1000220

Noori, N. A., & Ismail, Z. Z. (2019). Process optimization of biogas recovery from giant reed (Arundo donax) alternatively pretreated with acid and oxidant agent: Experimental and kinetic study. *Biomass Conversion and Biorefinery*, 1–15. https://doi.org/10.1007/s13399-019-00481-7

Okpokwasili, G. C., & Nweke, C. O. (2005). Microbial growth and substrate utilization kinetics. *African Journal of Biotechnology*, *5*(4), 305–317. http://www.academicjournals.org/AJB%0D

Olukanni, D. O., & Ojukwu, C. N. (2021). Biogas recovery from poultry and piggery waste. In *Biomethane through Resource Circularity* (1st ed., p. 13). CRC Press: Taylor and Francis Group.

Reynolds, J. (2016). Serial dilution protocols. *American Society for Microbiology*, 1–7.

Seekao, N., Sangsri, S., Rakmak, N., Dechapanya, W., & Siripatana, C. (2021). Co-digestion of palm oil mill effluent with chicken manure and crude glycerol: Biochemical methane potential by Monod kinetics. *Heliyon*, *7*(2), 1–17. https://doi.org/10.1016/j.heliyon.2021.e06204

Shariful Islam, M., Kabir, K. M. A., Tanimoto, J., & Saha, B. B. (2021). Study on Spirulina platensis growth employing non-linear analysis of biomass kinetic models. *Heliyon*, *7*, 1–9. https://doi.org/10.1016/j.heliyon.2021.e08185

Sieuwerts, S., Bok, F. A. M. De, Mols, E., Vos, W. M. De, & Vlieg, J. E. T. V. H. (2008). A simple and fast method for determining colony forming units. *Letters in Applied Microbiology*, *47*, 275–278. https://doi.org/10.1111/j.1472-765X.2008.02417.x

Spyridonidis, A., Vasiliadou, I. A., & Stamatelatou, K. (2022). Effect of zeolite on the methane production from chicken manure leachate. *Sustainability*, *14*(2207), 1–14. https://doi.org/10.3390/su14042207

Sule, I. O., Olorunfemi, A. A., & Otori, A. O. (2019). Mycological and bacteriological assessment of poultry droppings from poultry pens within Ilorin, Kwara, Nigeria. *Science World Journal*, *14*(4), 11–16. www.sciencewourldjournal.org

Syaichurrozi, I., & Rusdi, R. (2020). Development of simple kinetic model on biogas production from co-digestion of vinasse waste and tofu residue at variation of C/N Ratio. *World Chemical Engineering Journal*, *4*(1), 18–28. http://jurnal.untirta.ac.id/index.php/WCEJ

Tena, M., Perez, M., & Solera, R. (2021). Effect of hydraulic retention time on the methanogenic step of a two-stage anaerobic digestion system from sewage sludge and wine vinasse: Microbial and kinetic evaluation. *Fuel*, *296*(120674), 1–10. https://doi.org/10.1016/j.fuel.2021.120674

Tian, G., Yeung, M., & Xi, J. (2023). H2S emission and microbial community of chicken manure and vegetable waste in anaerobic digestion: A comparative study. In A. Siciliano (Ed.), *Fermentation* (Vol. 9, Issue 169, pp. 1–12). MDPI. https://doi.org/10.3390/fermentation9020169

UlukardeŞler, A. H., & Atalay, F. S. (2018). Kinetic studies of biogas generation using chicken manure as feedstock. *Journal of Polytechnic*, *0900*(4), 913–917. https://doi.org/10.2339/politeknik.389622

Um-e-Habiba, Khan, M. S., Raza, W., Gul, H., Hussain, M., Malik, B., Azam, M., & Winter, F. (2021). A study on the reaction kinetics of anaerobic microbes using batch anaerobic sludge technique for beverage industrial wastewater. *Separations*, *8*(43), 1–16. https://doi.org/10.3390/ separations8040043 Academic

Venkateshkumar, R., Shanmugam, S., & Veerappan, A. R. (2020). Anaerobic co-digestion of cow dung and cotton seed hull with different blend ratio: Experimental and kinetic study. *Biomass Conversion and Biorefinery*, 1–111. https://doi.org/10.1007/s13399-020-01006-3

Wahidah, M. P., Faiza, N. N., Nugraeni, C. D., & Purwanto, M. (2022). Small-scale biogas production: Utilization of chicken manure waste (Gallus gallus domesticus). *AIP Conference Proceedings 2638, 080003 (2022)*, *2638*(1). https://doi.org/10.1063/5.0104604

Yang, H., Deng, R., Jin, J., Wu, Y., Jiang, X., & Shi, J. (2021). Hydrolytic performances of different organic compounds in different lignocellulosic biomass during anaerobic digestion. *Environmental Engineering Resources*, *27*(4), 1–10. https://doi.org/10.4491/eer.2021.013

Yin, D. M., Uwineza, C., Sapmaz, T., Mahboubi, A., Wever, H. De, Qiao, W., & Taherzadeh, M. J. (2022). Volatile fatty acids (VFA) production and recovery from chicken manure using a high-solid anaerobic membrane bioreactor (AnMBR). *Membranes*, *12*(1133), 1–16. https://doi.org/10.3390/ membranes12111133

Zhai, H., & Qiang, H. (2022). Effect of tetracycline antibiotics on anaerobic digestion of chicken manure based on data mining. *Computational Intelligence and Neuroscience*, *6335146*, 1–12. https://doi.org/10.1155/2022/6335146

Ziganshina, E. E., & Ziganshin, A. M. (2022). Anaerobic digestion of chicken manure in the presence of magnetite, granular activated carbon, and biochar: Operation of anaerobic reactors and microbial community structure. *Microorganisms*, *10*(1422), 1–17. https://doi.org/10.3390/ microorganisms10071422